Effect of Spin-Orbit State on Chemical Reactivity: Study of Chemiluminescent and Ground-State Products from Reaction of $Sr(^3P_J^0)$ with Several Halogen-Containing Molecules

Mark L. Campbell[†] and Paul J. Dagdigian*

Contribution from the Department of Chemistry, The Johns Hopkins University, Baltimore, Maryland 21218. *Received January 10, 1986*

Abstract: Optical pumping state selection has been employed to study reactions of the $J = 0$ and 2 spin-orbit states of the $Sr(5s5p\ ^3P^0)$ manifold. The chemiluminescence cross sections for reaction of $Sr(^3P_2^0)$ with Cl_2, Br_2, CH_2Br_2, and CH_2I_2 are found to be at least 5-10 times larger than those of the $^3P_0^0$ state. Laser fluorescence detection was employed to study the spin-orbit dependence of the reaction pathway leading to ground-state SrBr products for $Sr(^3P^0)$ + HBr and CH_2Br_2. An opposite ordering of reactivity was found for this pathway, with $^3P_0^0$ being 2-3 times more reactive than $^3P_2^0$. These results, which are qualitatively and nearly quantitatively similar to our previous observations on $Ca(^3P^0)$ reactions, are discussed in terms of a dynamical model for understanding spin-orbit effects in chemical reactions.

It is now well established in the field of gas-phase chemical kinetics that different forms of reactant energy can have significantly different effects on chemical reactivity.[1] A large number of studies, both experimental and theoretical, have been carried out to probe the effect of rotational,[2-6] vibrational,[7-10] and electronic energy[11-13] in promoting chemical reactions. It has also been recognized that different spin-orbit states of a given electronic L-S term may exhibit differing reactivities, although there have been until recently relatively few studies in this area.

The importance of spin-orbit effects in chemical reactions might be expected to depend largely on the energy spacings in the multiplet. For heavy metals such as $Sn(^3P_J)$ and electronically excited $Hg(^3P_J^0)$, in which the spin-orbit spacings are comparable to energy differences between electronic terms, large spin-orbit dependences are anticipated and in fact observed.[14-18] Differing reactivities of the two metastable excited $^3P_{0,2}^0$ states of argon have been observed for the excimer formation and chemi-ionization channels in reactions with halogen compounds.[19,20] The altered ArX* excited state branching ratios have been explained as arising from the tendency to conserve the $Ar^+(^2P_{1/2,3/2}^0)$ core spin-orbit level during the collision.[19,20]

By contrast, for atomic reactants with small spin-orbit splittings, the different reactant spin-orbit states might be expected to be completely mixed in the entrance channel,[21] leading to a negligible spin-orbit dependence. However, adiabatic correlation arguments[22,23] in the strong spin-orbit coupling limit predict differing reactivities and product electronic state branching as a function of spin-orbit state in many reactions, regardless of the energy differences involved. For the F + HBr reaction it was possible to understand the low reactivity of the spin-orbit excited $^2P_{1/2}^0$ state through such arguments.[24] Likewise the excited $^2P_{1/2}^0$ state was found to be less reactive than the ground $^2P_{3/2}^0$ state in the $F + H_2$,[25,26] Br + HI,[27] and Br + IBr[28] reactions. Similar reasoning was also used to explain the absence of excited $I\ ^2P_{1/2}^0$ product in several halogen atom exchange reactions.[29-31] In some reactions, the height of the barrier on the adiabatic surface connecting spin-orbit excited reactant and product atoms is low enough to allow formation of excited product, e.g., $I^* + Br_2 \rightarrow IBr + Br^*$.[32-34]

For a number of years we have been interested in chemiluminescent reactions of ground and electronically excited alkaline earth atoms.[12,13,35] For these reactions, adiabatic correlation arguments are poor predictors of the observed electronic state branching ratios,[11-13,35,36] and there is evidence of strong mixing between different potential energy surfaces. In order to study the effect of incident spin-orbit state in these reactions, we have developed an optical pumping state selection method. In this technique, which we have thus far applied to the Ca $^3P_J^0$ manifold,[37-40] a single-mode cw dye laser is tuned to one line of a

[†] Permanent address: Department of Chemistry, U.S. Naval Academy, Annapolis, MD 21402.

(1) See, for example: Bernstein, R. B. *Chemical Dynamics via Molecular Beam and Laser Techniques*; Clarendon Press: Oxford, 1982.
(2) Zandee, L.; Bernstein, R. B. *J. Chem. Phys.* **1978**, *68*, 3760-3765.
(3) Altkorn, R.; Bartozek, F. E.; DeHaven, J.; Hancock, G.; Perry, D. S.; Zare, R. N. *Chem. Phys. Lett.* **1983**, *98*, 212-216.
(4) Man, C.-K.; Estler, R. C. *J. Chem. Phys.* **1981**, *75*, 2779-2785.
(5) Dispert, H. H.; Geis, M. W.; Brooks, P. R. *J. Chem. Phys.* **1979**, *70*, 5317-5319.
(6) Hoffmeister, M.; Potthast, L.; Loesch, H. J. *Chem. Phys.* **1983**, *78*, 369-380.
(7) Odiorne, T. J.; Brooks, P. R.; Kasper, J. V. V. *J. Chem. Phys.* **1971**, *55*, 1980-1982.
(8) Pruett, J. G.; Zare, R. N. *J. Chem. Phys.* **1976**, *64*, 1774-1783.
(9) Torres-Filho, A.; Pruett, J. G. *J. Chem. Phys.* **1982**, *77*, 740-747.
(10) Polanyi, J. C.; Schreiber, J. L. *Faraday Discuss. Chem. Soc.* **1977**, *62*, 267-290.
(11) Menzinger, M. *Adv. Chem. Phys.* **1980**, *42*, 1-61.
(12) Irvin, J. A. Dagdigian, P. J. *J. Chem. Phys.* **1981**, *74*, 6178-6187.
(13) Cox, J. W.; Dagdigian, P. J. *J. Phys. Chem.* **1982**, *86*, 3738-3745.
(14) Foo, P. D.; Wiesenfeld, J. R.; Yuen, M. J.; Husain, D. *J. Phys. Chem.* **1976**, *80*, 91-97.
(15) Felder, W.; Fontijn, A. *J. Chem. Phys.* **1978**, *69*, 1112-1120.
(16) Krause, H. F.; Johnson, S. G.; Datz, S.; Schmidt-Bleek, F. K. *Chem. Phys. Lett.* **1975**, *31*, 577-581.
(17) Hayashi, S.; Mayer, T. M.; Bernstein, R. B. *Chem. Phys. Lett.* **1978**, *53*, 419-422.
(18) Dreiling, T. D.; Setser, D. W. *J. Chem. Phys.* **1983**, *79*, 5423-5438.
(19) Golde, M. F.; Poletti, R. A. *Chem. Phys. Lett.* **1981**, *80*, 23-28. Golde, M. F.; Ho, Y.-S. *J. Chem. Phys.* **1985**, *82*, 3160-3168. Balamuta, J.; Golde, M. F.; Moyle, A. M. *J. Chem. Phys.* **1985**, *82*, *3169*-3178.
(20) Sadeghi, N.; Setser, D. W., private communication.
(21) This mixing during a reactive collision is to be distinguished from the fine-structure mixing which can occur in subsequent nonreactive collisions.
(22) Husain, D. *Ber. Bunsenges. Phys. Chem.* **1977**, *81*, 168-177.
(23) Brown, A.; Husain, D. *Can. J. Chem.* **1976**, *54*, 4-8.
(24) Hepburn, J. W.; Liu, K.; Macdonald, R. G.; Northrup, F. J.; Polanyi, J. C. *J. Chem. Phys.* **1981**, *75*, 3353-3364.
(25) Tully, J. C. *J. Chem. Phys.* **1974**, *60*, 3042-3050.
(26) Wyatt, R. E.; Walker, R. B. *J. Chem. Phys.* **1979**, *70*, 1501-1510.
(27) Bergmann, K.; Leone, S. R.; Moore, C. B. *J. Chem. Phys.* **1975**, *63*, 4161-4166.
(28) Haugen, H. K.; Weitz, E.; Leone, S. R. *Chem. Phys. Lett.* **1985**, *119*, 75-80.
(29) Das, P.; Venkitachalam, T.; Bersohn, R. *J. Chem. Phys.* **1984**, *80*, 4859-4862.
(30) Sung, J. P.; Setser, D. W. *Chem. Phys. Lett.* **1977**, *48*, 413-419.
(31) Maylotte, D. H.; Polanyi, J. C.; Woodall, K. *J. Chem. Phys.* **1972**, *57*, 1547-1560.
(32) Houston, P. L. *Chem. Phys. Lett.* **1977**, *47*, 137-141.
(33) Wiesenfeld, J. R.; Wolk, G. L. *J. Chem. Phys.* **1978**, *69*, 1797-1804, 1805-1813.
(34) Hofmann, H.; Leone, S. R. *J. Chem. Phys.* **1978**, *69*, 641-646.

0002-7863/86/1508-4701$01.50/0

multiplet ($^3S_1 \leftarrow {}^3P_J^0$) to depopulate a particular spin–orbit state and transfer its population to the other states of the manifold by radiative transitions.

The chemiluminescence cross section σ_{chem} for the reaction of $Ca(^3P_J^0)$ with Cl_2 and Br_2,[37] as well as a number of alkyl bromides[39] and iodides,[40] was found to depend strongly on initial spin–orbit level J, with a reactivity ordering of $J = 2 > J = 1 > J = 0$. Within the relatively large experimental errors, σ_{chem} for $J = 2$ was about 5–10 times greater than that for $J = 0$ for all these reactions. No spin–orbit dependence was found for $Ca(^3P_J^0) + SF_6$.[40] The reactive pathway leading to ground state $CaCl(X^2\Sigma^+)$ products was also investigated for $Ca(^3P_J^0) + Cl_2$, and the $J = 0$ level was found to have the largest cross section.[38] This selectivity is surprising in view of the relatively small $Ca(^3P_J^0)$ spin–orbit splittings (52 and 106 cm^{-1} [41]) and the expected strong mixing between different potential energy surfaces. The higher reactivity of the $^3P_0^0$ state was also found in a pseudoquenching model quantum scattering calculation.[42]

In the present paper, we use this state-selection technique to investigate the effect of the spin–orbit state on chemical reactivity for $Sr(5s5p\ ^3P_J^0)$, for which the spin–orbit spacings are somewhat larger:[41] $E(^3P_1^0 - {}^3P_0^0) = 187\ cm^{-1}$ and $E(^3P_2^0 - {}^3P_1^0) = 394\ cm^{-1}$. We have determined the spin–orbit dependence for the chemiluminescence pathway in the reaction of $Sr(^3P_J^0)$ with Cl_2, Br_2, CH_2Br_2, and CH_2I_2 and for the production of ground-state halide products in the $Sr(^3P_J^0) + CH_2Br_2$ and HBr reactions.

Experimental Section

A detailed description of the experimental apparatus has been given previously.[37,43] A beam of metastable electronically excited Sr atoms[13] was irradiated with a single-mode cw dye laser beam approximately 1 cm from the atomic beam source and passed through a collimating slit (3 × 6 mm) 26 cm downstream. The atoms then entered a scattering chamber to which reactant gases were introduced at pressures (measured with a capacitance manometer) of 0–0.8 mTorr. Emission of electronically excited products or laser fluorescence detection of nonemitting species was carried out in a zone 1.6 ± 0.1 cm downstream of the collimator. For the former, the chemiluminescence was observed with a 0.25-m spectrometer and cooled photomultiplier (RCA C31034-02), while the latter measurements employed a homemade grazing-incidence pulsed dye laser[44] pumped by an excimer laser (Lambda Physik EMG53MSC).

The strontium atom has two metastable states,[41] $5s5p\ ^3P_J^0$ and $5s4d\ ^1D_2$, both of which are produced in our discharge atomic beam source. The short radiative lifetime of the $^3P_1^0$ state (20.1 ± 0.4 μs[45]) coupled with the long source-to-scattering chamber distance essentially rendered the $^3P^0$ multiplet a two-level ($^3P_{0,2}^0$) rather than three-level system, greatly simplifying the determination of spin–orbit-dependent cross sections. In order to measure the latter, the spin–orbit populations were altered by optical depletion of the $^3P_0^0$ level through irradiation of the Sr* beam by the cw laser (CR599-21 with DCM II dye) tuned to the $5s6s\ ^3S_1 \leftarrow 5s5p\ ^3P_0^0$ line at 679.3 nm. Because of its larger incident population, pumping of the $^3P_2^0$ state would reduce the experimental errors in the determination of cross sections; however, the dye laser could not be tuned far enough to the red to reach the $^3S_1 \leftarrow {}^3P_2^0$ line at 707.2 nm.

In our previous experiments with Ca,[37-40] the cw laser wavelength was centered on the pumping transition by observing the change in the beam $^3P_1^0 \rightarrow {}^1S$ emission intensity. This method could not be used here because of the short $^3P_1^0$ radiative lifetime. Instead, a laser fluorescence detector was set up in the scattering chamber 78 cm downstream of the source.

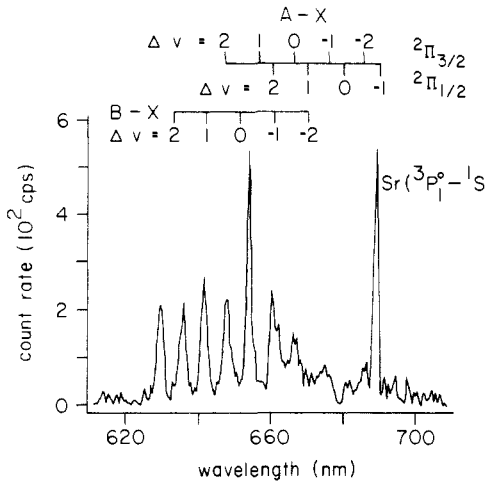

Figure 1. Chemiluminescence spectrum of the SrBr A–X and B–X band systems for the reaction of metastable Sr with Br_2 at 0.49 mTorr scattering gas presssures. The vibrational sequences $\Delta v = v' - v''$ for each band system (taken from ref 55 and 56) are marked. Spectrometer slit width was 250 μm.

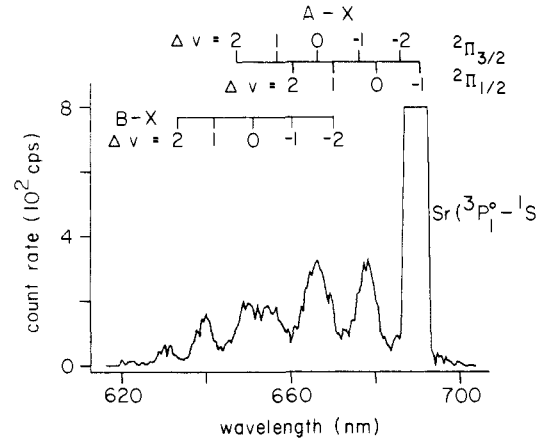

Figure 2. Chemiluminescence spectrum of the SrBr A–X and B–X band systems for $Sr^* + CH_2Br_2$ at 0.46 mTorr. Spectrometer slit width was 1000 μm.

A small fraction of the cw laser radiation was directed to this detector, and the wavelength was optimized by maximizing the $^3S_1 \leftarrow {}^3P_0^0$ laser fluorescence signal.

Laser fluorescence measurements were carried out to determine the relative populations of the states in the incident Sr* beam. These observations were made at the same place that the reactions were detected. The populations of the $^3P_J^0$ spin–orbit levels were obtained by comparing the fluorescence signals excited by the pulsed dye laser on the $5s7s\ ^3S_1 \leftarrow 5s5p\ ^3P_{0,1,2}^0$ lines at 432.8, 436.3, and 443.9 nm, respectively.[46] For these measurements, the pulsed dye laser was attenuated with neutral density filters so that the fluorescence signal was linear with laser power. Simultaneous measurements of the laser pulse energy were also made, and the fluorescence signal normalized to constant energy. With the cw pump laser off, the relative spin–orbit populations were determined to

(35) Alexander, M. H.; Dagdigian, P. J. *Chem. Phys.* **1978**, *33*, 13–25.
(36) Kowalski, A.; Menzinger, M. *Chem. Phys. Lett.* **1981**, *78*, 461–466. Menzinger, M. In *Gas-Phase Chemiluminescence and Chemi-Ionization*; Fontijn, A., Ed.; North-Holland: Amsterdam, 1985; pp 25–68.
(37) Yuh, H.-J.; Dagdigian, P. J. *J. Chem. Phys.* **1984**, *81*, 2375–2384.
(38) Dagdigian, P. J. In *Gas-Phase Chemiluminescance and Chemi-Ionization*; Fontijn, A., Ed.; North-Holland: Amsterdam, 1985; pp 203–219.
(39) Furio, N.; Campbell, M. L.; Dagdigian, P. J. *J. Chem. Phys.* **1986**, *84*, 4332–4340.
(40) Campbell, M. L.; Furio, N.; Dagdigian, P. J. *Laser Chem.*, in press.
(41) Moore, C. E. *Atomic Energy Levels*; Natl. Bur. Stand. Ref. Data Ser. Natl. Bur. Stand. 35; U.S. Government Printing Office: Washington, DC, 1971; Vol. II.
(42) Alexander, M. H. In *Gas-Phase Chemiluminescence and Chemi-Ionization*; Fontijn, A., Ed.; North-Holland: Amsterdam, 1985; pp 221–238.
(43) Yuh, H.-J.; Dagdigian, P. J. *Phys. Rev. A* **1983**, *28*, 63–72.
(44) Littman, M. G.; Metcalf, H. J. *Appl. Opt.* **1978**, *17*, 2224–2227.
(45) Husain, D.; Schifino, J. *J. Chem. Soc., Faraday Trans. 2* **1984**, *80*, 321–334.
(46) Radiative transition probabilities were taken from: Eberhagen, A. *Z. Phys.* **1955**, *143*, 392–411.
(47) Chase, M. W.; Curnutt, J. L.; Prophet, H.; McDonald, R. A.; Syverud, A. N. *J. Phys. Chem. Ref. Data* **1975**, *4*, 1–175.
(48) Hildenbrand, D. L. *J. Chem. Phys.* **1977**, *66*, 3526–3529.
(49) Kleinschmidt, P. D.; Hildenbrand, D. L. *J. Chem. Phys.* **1978**, *68*, 2819–2824.
(50) Estler, R. C.; Zare, R. N. *Chem. Phys.* **1978**, *28*, 253–263.
(51) Chase, M. W.; Curnutt, J. L.; Hu, A. T.; Prophet, H.; Syverud, A. N.; Walker, L. C. *J. Phys. Chem. Ref. Data*, **1974**, *3*, 311–480.
(52) Barrow, R. F.; Clark, T. C.; Coxon, J. A.; Yee, K. K. *J. Mol. Spectrosc.* **1974**, *51*, 428–449.
(53) Darwent, B. de B. *Bond Dissociation Energies in Simple Molecules*; Natl. Bur. Stand. Ref. Data Ser. Natl. Bur. Stand. 31; U.S. Government Printing Office: Washington, DC, 1970.
(54) Dagdigian, P. J.; Cruse, H. W.; Zare, R. N. *Chem. Phys.* **1976**, *15*, 249–260.

Table I. Reaction Energetics (in eV) for the Sr + RX → SrX + R Reactions

RX	ΔD_0[a]	E_{int}(RX),[b]	E_{trans}[c]	E_{avl}(^{1}S),[d]	E_{avl}(^{3}P^0)[d]
Cl_2	1.73 ± 0.09[e]	0.03	0.13 ± 0.02	1.89	3.73
Br_2	1.44 ± 0.10[f]	0.04	0.17 ± 0.02	1.65	3.49
CH_2Br_2	0.81 ± 0.16[g]	0.07	0.18 ± 0.02	1.06	2.90
CH_2I_2	0.58 ± 0.11[h]	0.07	0.20 ± 0.02	0.85	2.69
HBr	−0.35 ± 0.10[i]	0.03	0.14 ± 0.02	−0.18[j]	1.66

[a] D_0^0(SrX) − D_0^0(RX). The strontium halide bond energies employed are D_0^0(SrCl) = 4.21 ± 0.09 eV,[47] D_0^0(SrBr) = 3.41 ± 0.10 eV,[48] and D_0^0(SrI) = 2.76 ± 0.06 eV.[49] [b] Internal energy of the halide reagent. [c] Average initial relative translational energy, computed by convoluting the beam[13] and target gas velocity distributions (see ref 50). The Sr velocity distribution here is somewhat colder than that measured in ref 13 because the beam is much less supersonic. [d] E_{avl}(^{1}S) and E_{avl}(^{3}P^0) are the total energy available to the products for the ^{1}S and ^{3}P^0 reactions, respectively. E_{avl} equals ΔD_0 + E_{int}(RX) + E_{trans}[i] + E_{int}(Sr). E_{int}(Sr) = 0, 1.835, and 2.498 eV for the ^{1}S, ^{3}P^0, and ^{1}D states, respectively.[41] [e] Reference 51. [f] Reference 52. [g] Reference 53. [h] Reference 54. [i] Reference 47. [j] Reaction is endoergic.

be 0.83 ± 0.02, 0.001 ± 0.001, and 0.17 ± 0.02 for the J = 2, 1, and 0 states, respectively. The effect of optical pumping on the relative spin-orbit populations was measured by observing the change in the pulsed laser fluorescence signal corresponding to detection of a given spin-orbit state upon cw laser depletion of the $^3P_0^0$ state. We find that optical pumping removes all but about 5% of the original $^3P_0^0$ population, at incident laser powers of 50–90 mW in a 0.4-cm-diameter beam. With the pump laser on, the relative populations become 0.93 ± 0.02, 0.001 ± 0.001, and 0.01 ± 0.01. These populations have been normalized so that the total $^3P^0$ population equals unity when the cw laser is off. It should be noted that the total $^3P^0$ population is slightly reduced when the $^3P_0^0$ state is depleted because a fraction of the $^3P_0^0$ atoms optically excited radiate to the $^3P_1^0$ state, which rapidly decays to the ground ^{1}S state. In reporting these populations, account was taken of the ^{87}Sr isotope, which is not optically pumped by the narrow-band cw laser but is detected along with the predominant ^{88}Sr isotope by the pulsed probe laser.

Our previous studies of Ca* reactions[39,40] showed that reactions of the ^{1}D metastable state can yield a significant fraction of the observed chemiluminescence. The ^{1}D/^{3}P^0 population ratio here was determined to be 5 ± 2% by comparison of ^{3}P^0 laser fluorescence signals with signals at the 5s10p ^{1}P^0, 5s6f ^{1}F^0, and 5s9p ^{1}P^0 ← 5s4d ^{1}D transitions at 431.4, 440.7, and 448.2 nm, respectively. Unlike for Ca, it was not possible to measure the fraction of the chemiluminescence due to the ^{1}D reaction by optical depletion of the ^{1}D state since the relevant pumping transition (5s6p ^{1}P^0 ← 5s4d ^{1}D line at 716.9 nm) is too far to the red to be reached by our cw dye laser. However, the Sr ^{1}D/^{3}P^0 population ratio is considerably less than that in our Ca* studies so that the ^{1}D reactions should be less important here.

Results

Chemiluminescent Reaction Products. For most of the reactants, the exoergicity with the Sr(^{3}P^0) incident level is sufficiently large to allow direct production of the SrX A and B electronic states (see Table I). Figures 1–3 present chemiluminescence spectra for the reactions of Sr* with Br_2, CH_2Br_2, and CH_2I_2. The spectrum obtained for Sr* + Cl_2 was essentially identical with that obtained previously with higher spectral resolution.[55] Our spectra were taken under relatively low resolution so that only vibrational sequences of the A–X and B–X band systems[55-58] are observed. The SrI A and B states lie very close in energy[57] so that the SrI A–X and B–X band systems cannot be separated in the Sr* + CH_2I_2 spectrum.

The chemiluminescence spectra in Figures 1 and 2 for the Sr* + Br_2 and CH_2Br_2 reactions are significantly different, even allowing for the different spectral resolutions with which the spectra were taken. This suggests dissimilar SrBr* product vibrational excitation, as would be expected from the differing exoergicities (see Table I). The most prominent features are the Δv = 0 sequences for Sr* + CH_2Br_2 (Figure 2), while a significant portion of the emission is in the off-diagonal sequences (particularly Δv = +1 and +2) for Sr* + Br_2. Because these electronic transitions involve the promotion of a nonbonding electron,[59] the

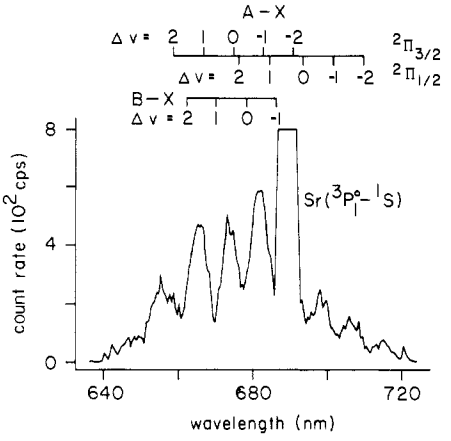

Figure 3. Chemiluminescence spectrum of the SrI A–X and B–X band system for Sr* + CH_2I_2 at 0.47 mTorr. Spectrometer slit width was 1000 μm. Band-head positions were taken from ref 57.

Franck–Condon arrays are expected to be diagonal for low vibrational quantum numbers. However, as the vibrational excitation increases, off-diagonal sequences will become more important. Thus, we infer from Figures 1 and 2 a higher SrBr* vibrational excitation from the Sr* + Br_2 reaction than for Sr* + CH_2Br_2, although it is not possible to make quantitative estimates for either reaction.

In our previous studies,[12,13,37,39,40] we were able to determine absolute chemiluminescence cross sections by comparison of the emission intensities of the chemiluminescent products and the radiating reactants. However, because of the short $^3P_1^0$ radiative lifetime[45] and long source-to-observation-zone distance, the $^3P_1^0$ → ^{1}S emission signal at 689.4 nm does not accurately reflect the $^3P^0$ population. This signal arises almost entirely from collisional intramultiplet mixing from the other spin-orbit levels. As evidence for this, we note that when the $^3P_1^0$ was optically pumped with the cw laser tuned to the $^3S_1$ ← $^3P_1^0$ transition at 688.0 nm, the $^3P_1^0$ → ^{1}S emission signal actually increased slightly, while this signal decreased when the $^3P_0^0$ level was optically pumped. Furthermore, the emission intensity was observed to be largely dependent on the scattering chamber base pressure.

Even though absolute chemiluminescence cross sections could not be calculated, comparison of integrated chemiluminescence intensities indicates that the cross sections for the Cl_2 and Br_2 reactions are about ≥5 times greater than for CH_2Br_2 and CH_2I_2. These relative values are similar to those observed for the corresponding Ca reactions.[39,40]

To determine the dependence of the chemiluminescence cross sections on reagent spin-orbit state, the change in the emission intensity when the $^3P_0^0$ was optically pumped was recorded. To minimize the scrambling due to collisional intramultiplet mixing, the scattering gas pressures were kept below 0.6 mTorr. With the cw laser off, the chemiluminescent signal S_{SrX} can be expressed as

$$S_{SrX} = k(0.17\sigma_0 + 0.83\sigma_2) \quad (1)$$

where σ_J is the chemiluminescence cross section for Sr $^3P_J^0$ atomic reactant and k is a proportionality constant which includes the

(55) Brinkmann, U.; Schmidt, V. H.; Telle, H. *Chem. Phys. Lett.* **1980**, *73*, 530–535. Brinkmann, U.; Schmidt, V. H.; Telle, H. *Chem. Phys.* **1982**, *64*, 19–41.
(56) Schröder, J. O.; Ernst, W. E. *J. Mol. Spectrosc.* **1985**, *112*, 413–429.
(57) Harrington, R. E. Ph.D. Thesis, University of California, Berkeley, 1942.
(58) Ashrafunnisa; Rao, D. V. K.; Rao, P. T. *J. Phys. B* **1973**, *6*, 1503–1509.
(59) See, for example, Rice, S. F.; Martin, H.; Field, R. W. *J. Chem. Phys.* **1985**, *82*, 5023–5034.

Table II. Observed Changes R_c in Reaction Product Signals when the $Sr(^3P_0^o)$ State is Optically Depleted

reagent	ground-state product	chemiluminescence signal A–X	B–X
Cl_2	*a*	1.090 ± 0.006	1.075 ± 0.015
Br_2	*a*	1.084 ± 0.004	1.083 ± 0.006
CH_2Br_2	0.82 ± 0.01	1.08 ± 0.01	*a*
CH_2I_2	*a*	1.096 ± 0.012[b]	
HBr	0.71 ± 0.01	*c*	*c*

[a] Not measured. [b] SrI A and B states not resolvable. [c] Not energetically accessible.

Table III. Ratio σ_0/σ_2 of Cross Sections for Production of Specific SrX Product Electronic States

reagent	σ_0/σ_2 X $^2\Sigma^+$	A $^2\Pi$	B $^2\Sigma^+$
Cl_2	*a*	0.14 ± 0.17	0.22 ± 0.19
Br_2	*a*	0.17 ± 0.17	0.18 ± 0.17
CH_2Br_2	1.93 ± 0.36[b]	0.19 ± 0.18	*a*
CH_2I_2	*a*	0.12 ± 0.18[c]	
HBr	3.08 ± 0.54	*d*	*d*

[a] Not measured. [b] Lower limit because of cascade contribution from chemiluminescence channels. [c] SrI A and B states not resolved. [d] Not energetically accessible.

total number densities of the reagents, detector quantum efficiency and geometrical viewing factors, etc. We have included in eq.1 the relative incident spin-orbit populations reported in the Experimental section. The ^1D reaction has also been assumed to produce a negligible contribution to the chemiluminescence.

When the $^3P_0^0$ state is optically depleted, the signal changes by a factor R_0, and the observed signal S'_{SrX} can be expressed as

$$S'_{SrX} = R_0 S_{SrX} = k(0.01\sigma_0 + 0.93\sigma_2) \quad (2)$$

Equations 1 and 2 can be solved to yield directly the ratio σ_0/σ_2 of the chemiluminescence cross sections with $J = 0$ and 2 reactants:

$$\sigma_0/\sigma_2 = (0.93 - 0.83R_0)/(0.17R_0 - 0.01) \quad (3)$$

Spin–orbit effects were studied for the chemiluminescent pathway of the $Sr(^3P^0)$ reaction with Br_2, Cl_2, CH_2Br_2, and CH_2I_2. In all cases, the spectra exhibited no noticeable change in shape when the $^3P_0^0$ state was optically depleted. However, the chemiluminescence intensities significantly increased when the pump laser was turned on. Table II presents the measured R_0 values for the reactions studied; within the experimental errors all the ratios are the same.

The data in Table II were used with eq 3 to calculate the cross-section ratios σ_0/σ_2, which are reported in Table III. The reported uncertainties were obtained from a propagation of errors treatment.[60] The principal source of error in these measurements arises from the uncertainties in the $Sr(^3P^0)$ spin–orbit populations. The effect of initial spin–orbit state on the A–X and B–X chemiluminescence pathways for the four reactions studied are similar and substantial. The $J = 2$ spin–orbit state is much more reactive for this pathway than the $J = 0$ state, with σ_2 at least 5 times greater than σ_0. This ratio is actually a lower limit because it was not possible to measure the contribution of the ^1D reactions to the observed SrX product signals. However, in view of the smaller $^1D/^3P^0$ population ratio for Sr* in these experiments as compared to this ratio in our earlier Ca* studies,[39] we estimate the neglect of the ^1D reaction to contribute a systematic error to σ_0/σ_2 roughly equal to the uncertainities reported in Table III. Here we have assumed the ratio of the Sr ^1D and $^3P^0$ chemiluminescence cross sections is comparable to that previously measured[39,40] for the corresponding Ca* reactions. The uncertainties in σ_0/σ_2 could be significantly reduced if the $^3P_2^0$, rather than $^3P_0^0$, spin–orbit level were optically pumped because of the much higher incident population in the former.

(60) Bevington, P. R. *Data Reduction and Error Analysis for the Physical Sciences*; McGraw-Hill: New York, 1969.

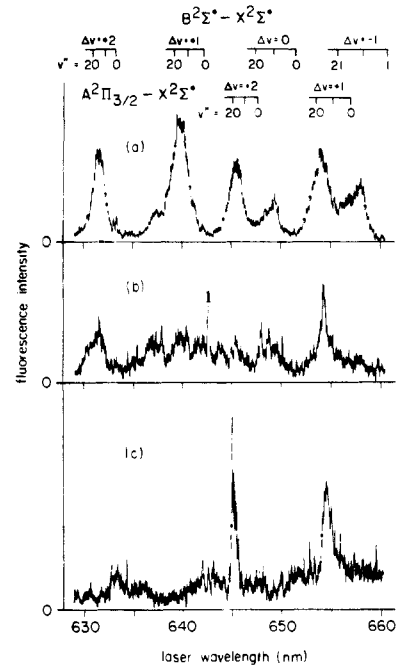

Figure 4. Laser fluorescence excitation spectrum from 630 to 660 nm of the SrBr A–X and B–X band systems for the (a) Sr + CH_2Br_2, (b) Sr* + CH_2Br_2, and (c) Sr* + HBr reactions. The scattering gas pressure was (a) 0.68, (b) 0.70, and (c) 0.50 mTorr, respectively. The ordinate scale is arbitrary, and relative intensities of the different spectra cannot be compared.

Ground-State Reaction Products. The SrBr reaction product formed in the ground $X^2\Sigma^+$ electronic state was investigated by laser fluorescence detection in the A–X and B–X band systems for the Sr* + HBr and CH_2Br_2 reactions. For the latter, formation of ground-state products is energetically allowed for ground ^1S atomic reactant, as well as for the metastable excited levels (see Table I). Figure 4 presents laser fluorescence excitation spectra for the reaction of CH_2Br_2 with (a) ground-state and (b) metastable excited Sr atoms taken under single-collision conditions. The vibrational sequences of the A–X and B–X band systems are clearly observable in the $Sr(^1S) + CH_2Br_2$ spectrum. In slower scans, individual band heads are also discernable. Previous studies of analogous reactions, both by laser fluorescence[61,62] and crossed-beam mass spectrometric studies,[63] suggest that a substantial fraction of the exoergicity will appear as SrBr internal excitation. We have not attempted a detailed analysis of the spectrum to extract a vibrational distribution. However, from the shape of the sequence features, the distribution appears inverted, with a maximum population near $v = 18 \pm 2$; the energy of this level represents 45% of $E_{avl}(^1S)$.

The spectrum in Figure 4b for Sr* + CH_2Br_2 is considerably different than that in Figure 4a. The features corresponding to the $Sr(^1S)$ reaction are considerably reduced in intensity because of the conversion of ground-state atoms to the metastable $Sr(^3P^0,^1D)$ excited levels in the discharge within the atomic beam source. The most prominent features in the spectrrum at 642.6 and 654.1 nm are due to highly vibrationally excited SrBr products from the excited-state reactions. Note that $E_{avl}(^3P^0)$ represents about 78% of the SrBr bond energy so that the reaction products can be produced with substantial internal excitation. We hesitate to assign these features in Figure 4b to particular vibrational sequences because the SrBr band systems have been analyzed only for low vibrational bands.[56,57] By analogy with SrCl,[55] heads of heads are expected to occur in many sequences so that it is not

(61) Rommel, M.; Schultz, A. *Ber. Bunsenges. Phys. Chem.* **1977**, *81*, 139–142.
(62) Chakravorty, K. K.; Bernstein, R. B. *J. Phys. Chem.* **1984**, *88*, 3465–3472.
(63) Lin, S.-M.; Mims, C. A.; Herm, R. R. *J. Phys. Chem.* **1973**, *77*, 569–575.

possible to extrapolate the band positions to high vibrational levels.

Figure 4c illustrates the laser fluorescence spectrum for Sr* + HBr. The ground-state $Sr(^1S)$ + HBr reaction is endoergic, and no reaction product was detected when the discharge in the beam source was turned off. The SrBr spectrum in Figure 4c is very similar to that in Figure 4b for the corresponding CH_2Br_2 reaction, with prominent features at 644.8 and 654.4 nm.

While we cannot assign the features observed in the laser fluorescence spectra for the Sr* reactions, we may nevertheless measure the changes in intensity upon $^3P_0^0$ optical pumping to determine the effect of incident spin–orbit state on the ground-state reaction product pathways. The $Sr(^3P^0)$ + HBr reaction is particularly convenient for study since the corresponding $Sr(^1S)$ reaction is endoergic. Hence, no correction needs to be made for the latter, as was necessary in our study[38] of $Ca(^3P^0)$ + Cl_2. Also, there is no chemiluminescence to obscure the laser fluorescence signal. The change R_0 in the laser fluorescence signal when the $^3P_0^0$ atomic state was optically depleted was measured at two laser excitation wavelengths (644.8 and 654.4 nm) for the $Sr(^3P^0)$ + HBr reaction. The R_0 ratios determined were identical within experimental error; the resulting value is reported in Table II. Equation 3 was then used to determine the ratio σ_0/σ_2 of cross sections for formation of ground-state products from the $^3P_0^0$ and $^3P_2^0$ reactant states; the derived value of σ_0/σ_2 is presented in Table III. We have assumed that the ^1D reaction yields negligible ground-state SrBr product.

The determination of the spin–orbit effect for the ground-state reaction pathway of $Sr(^3P^0)$ + CH_2Br_2 is complicated by ground-state products from the exoergic $Sr(^1S)$ + CH_2Br_2 reaction, as well as radiative decay of chemiluminescent products into the ground electronic state. The contribution of the ^1S reaction to the observed SrBr laser fluorescence signal was determined in the following way. The reduction in the $Sr(^1S)$ concentration in the atomic beam when the discharge in the source was turned on was measured by observing the change in the laser fluorescence signal excited by the $^1P^0 \leftarrow {}^1S$ line at 460.9 nm with no scattering gas present. It was found that the ^1S density is reduced to 45 ± 5% of its original value when the discharge is turned on. The SrBr product laser fluorescence signal was measured with the source discharge off, and 45% of that signal was subtracted from the corresponding signal measured with the discharge on to correct for the contribution from the ^1S reaction.

The change R_0' in the laser fluorescence signal upon $^3P_0^0$ optical depletion without correction for the ^1S reaction was measured to be 0.83 ± 0.01 and 0.90 ± 0.01 at laser excitation wavelengths 642.6 and 654.1 nm, respectively. The larger R_0' value at the latter wavelength reflects the greater ^1S contribution to the laser fluorescence signal (see Figure 4). The corrected ratio R_0 for 642.6 nm is reported in Table II. This result was deemed more reliable than that for 654.1 nm because of the smaller ^1S contribution. However, R_0 for the latter (0.85 ± 0.03) was virtually identical but with a larger uncertainty. In Table III we report the cross-section ratio σ_0/σ_2, obtained by using eq 3, for this reaction pathway. We see that for both $Sr(^3P^0)$ + HBr and CH_2Br_2 the dependence of the cross section on incident spin–orbit level for the formation of ground state products is opposite to that for the chemiluminescence pathway. For the former, the $^3P_0^0$ state has a larger cross section than for $^3P_2^0$, as was also found previously for $Ca(^3P^0)$ + Cl_2.[38] Because of the opposite ordering of reactivity, the cascade contribution to the ground-state SrBr product signal from the chemiluminescence pathway will alter the σ_0/σ_2 ratio observed for the ground-state product pathway. We expect this to be only a small correction because most reactive events lead to products in the ground electronic state.[11,39,40]

Discussion

In this paper, we have found that the dependence of reactivity on incident spin–orbit state for the $Sr(5s5p\ ^3P^0)$ manifold is similar qualitatively and nearly quantitatively to that previously seen for the analogous $Ca(4s4p\ ^3P^0)$ multiplet,[37-40] at least for reactions involving simple halide reagents. Specifically, the chemiluminescence cross sections for reaction of $Sr(^3P_J^0)$ with Cl_2, Br_2, CH_2Br_2, and CH_2I_2 are found to be at least 5–10 times larger for the higher energy $J = 2$ spin–orbit level than for $J = 0$. An opposite ordering of reactivity was found for the reaction pathway leading to ground-state SrBr products in the $Sr(^3P^0)$ + HBr and CH_2Br_2 reactions. Here the $^3P_0^0$ spin–orbit level has a reaction cross section 2–3 times larger, depending on the reaction, than for $^3P_2^0$. This reversal of reactivity confirms a similar, but less precise, observation[38] for $Ca(^3P^0)$ + Cl_2.

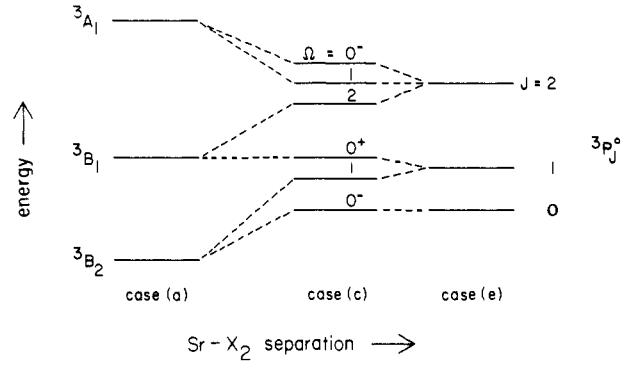

Figure 5. Correlation diagram for the interaction of $Sr(^3P^0)$ with a diatomic halogen molecule in the preferred C_{2v} geometry, illustrating the connection between the case e states at large separations with the case a states.

Because of the relatively low ionization potential of $Sr(^3P^0)$, the dynamics of these reactions are expected to involve charge transfer to an ionic surface. As $Sr(^3P^0)$ approaches the reactant, but before charge transfer has occurred, electrostatic interactions will cause a splitting into several covalent surfaces, depending on the orientation of the unpaired p electron of the metal atom with respect to the nuclear framework.[36,37] When the separation between the reagents is large, the atomic spin–orbit splitting is greater than either the electrostatic interaction between the reactants or the rotational (centrifugal) energy so that the atomic $\vec{L}$ and $\vec{S}$ vectors couple to form $\vec{J}$, which remains a good quantum number, defining a Hund's case e representation.[64] At smaller separations, the electrostatic interaction becomes dominant, and the wavefunctions are better described by a Hund's case a basis,[64] wherein the projections of angular momenta along a molecular axis are well defined. Conceptually at least, we can think of the transformation from case e to case a as occurring via a case c representation, as illustrated in Figure 5 for the interaction with a diatomic halogen molecule in the preferred C_{2v} approach geometry. We see that the lower energy spin–orbit states adiabatically correlate with the lower energy electrostatic surfaces. In Alexander's pseudoquenching model calculation[42] on $Ca(^3P^0)$ + Cl_2, such adiabatic correlations represented reasonably the ordering of reactivity of the spin–orbit levels, in spite of the relatively small fine-structure splitting. Since the different electrostatic surfaces are expected to display different reactivities, the evolution of the $^3P_J^0$ states to differing mixtures of case a states will lead to an observed spin–orbit effect in a chemical reaction.

The reversal of spin–orbit reactivity for the chemiluminescence and ground-state reaction pathways can be explained as arising from the selective removal of flux at the outermost ionic–covalent crossing. Chemiluminescent products are formed in those encounters for which this crossing in traversed without electron transfer and excited ionic surfaces are accessed.[36,37] Since $^3P_2^0$ reactants yield ground-state products with lowest probability, they are most likely to reach these ionic surfaces, from which electronically excited products are formed. Because of the multitude of excited ionic surfaces correlating to excited $M(np,(n-1)d)^+$ ions, we do not expect any symmetry restrictions at the crossings of the covalent and excited ionic surfaces.

It is interesting to speculate on the differences we might expect for the spin–orbit dependence of atomic reactants of different

(64) Herzberg, G. *Molecular Spectra and Molecular Structure. I. Spectra of Diatomic Molecules*; D. Van Nostrand: Princeton, 1950.

fine-structure splittings. Since the reagents approach one another with a finite velocity, the wavefunction corresponding to a single incident spin-orbit level nonadiabatically builds up amplitude on more than one electrostatic surface at smaller separations. In nonreactive systems this mixing causes collisional transitions between the fine-structure levels.[65,66] In a semiclassical description of this process,[42,65,66] the range of separations at which this mixing occurs is around that for which the electrostatic splittings equal the spin-orbit splittings. Since the latter is larger for $Sr(^3P^0)$ than for $Ca(^3P^0)$, the nonadiabatic mixing arises at smaller separations for Sr. In the extreme case of $Hg(^3P^0)$ the spin-orbit splitting is so large that the collisions are almost entirely adiabatic.[15-17] We would thus expect the spin-orbit effect in $Sr(^3P^0)$ reactions to be larger than those involving $Ca(^3P^0)$.

Unfortunately, the experimental errors are large, but at least for the ground-state reaction pathway it appears that there is a somewhat greater spin-orbit selectivity in $Sr(^3P^0)$ reactions, if the present results are compared with the previous results[38] for $Ca(^3P^0) + Cl_2$. For the chemiluminescence pathway, the dependence on spin-orbit state appears quite similar to within experimental error for all the $Ca(^3P^0)$[37,39,40] and $Sr(^3P^0)$ reactions studied, with the one exception of $Ca(^3P^0) + SF_6$, for which all the spin-orbit levels had about the same chemiluminescence cross section.[40] Perhaps more precise measurements of the spin-orbit dependent cross sections would reveal some differences between the $Ca(^3P^0)$ and $Sr(^3P^0)$ reactions.

Acknowledgment. Dr. Nick Furio constructed the dye laser used for the laser fluorescence measurements. This work was supported by the National Science Foundation under Grant CHE-8400014.

Registry No. Sr, 7440-24-6; Cl_2, 7782-50-5; Br_2, 7726-95-6; CH_2Br, 74-95-3; CH_2I_2, 75-11-6.

(65) Nikitin, E. E. *Adv. Chem. Phys.* **1975**, *28*, 317-377.
(66) Alexander, M. H.; Orlikowski, T.; Straub, J. E. *Phys. Rev. A* **1983**, *28*, 73-82.

Temperature Dependence of the Lifetime of Excited Benzyl and Other Arylmethyl Radicals‡

Dan Meisel,*† Paritosh K. Das,§ Gordon L. Hug,§ Kankan Bhattacharyya,§ and Richard W. Fessenden*§

Contribution from the Chemistry Division, Argonne National Laboratory, Argonne, Illinois 60439, and the Radiation Laboratory and Department of Chemistry, University of Notre Dame, Notre Dame, Indiana 46556. *Received January 13, 1986*

Abstract: The temperature dependence of the fluorescence lifetime of benzyl, benzyl-d_7, α-methylbenzyl, and triphenylmethyl radicals has been studied in 2-methyltetrahydrofuran from 77 to 300 K. Temperature independent and unusual temperature dependent relaxation pathways are observed for the excited states of all four radicals. Activation energies for the temperature-dependent relaxation process are $\sim$1400 cm^{-1} for all these radicals, and frequency factors are in the range of (2-20) $\times 10^{11}$ s^{-1}. For Ph_3C radicals, the temperature-dependent process leads to observable photochemistry. However, no photochemistry is observed to result from the thermally activated relaxation of benzyl radicals. Possible pathways of these nonradiative decay processes are discussed and contrasted with the weak temperature dependence for the relaxation of diphenylmethyl radicals. It is proposed that the temperature-dependent route for the radiationless decay of benzyl radicals results from differential vibronic mixing of the two excited states, the 1^2A_2 and 2^2B_2 states. Most efficient in that mixing seems to be C-C stretching vibrational modes.

Photophysics and photochemistry of short-lived radicals in liquid solutions have recently become a focus of renewed interest.[1-7] In a typical experiment, radicals for such studies are produced by a preliminary pulse (using either pulse radiolysis[1,2] or laser flash photolysis[3-6]) and are excited shortly thereafter by another laser pulse. With use of such a double-pulse technique, the photophysics and photochemistry of a series of arylmethyl radicals have been recently studied in a variety of liquids at room temperature.[1,2,5] These studies revealed that the lowest excited doublet state of diphenylmethyl, $Ph_2\dot{C}H^*$, is remarkably long lived and is highly emissive (τ = 280 ns, Φ_{fl} = 0.3). While no intramolecular photochemistry was observed for $Ph_2\dot{C}H^*$, high yields of intramolecular photochemistry ($\phi_{Ph} \sim 1$) were observed for the substituted $Ph_2\dot{C}R^*$ (R = Ph, Me, or c-Pr) radicals. An electrocyclic ring closure, resulting from an increased twist angle of the phenyl rings out of the central molecular plane, has been proposed[8] to rationalize these striking differences between $Ph_2\dot{C}H^*$ and $Ph_2\dot{C}R^*$.[1,2,9] Further studies have shown that neither the radiative nor the nonradiative decay rates of $Ph_2\dot{C}H^*$ change appreciably upon decreasing the temperature down to 77 K (in 2-methylpentane/cyclohexane glass).[9] On the other hand, for $Ph_2\dot{C}R^*$ fluorescence quantum yields in the glassy matrix at 77 K are significantly higher than those for $Ph_2\dot{C}H^*$ primarily due to higher radiative decay rates. However, at room temperature and in the

‡Work performed under the auspices of the Office of Basic Energy Sciences, Division of Chemical Sciences, U.S. Department of Energy, under contract No. W-31-109-ENG-38 (ANL) and No. DE-AC02-76ER00038 (NDRL). This is also Document No. NDRL-2816 of the Notre Dame Radiation Laboratory.
†Argonne National Laboratory.
§University of Notre Dame.

(1) Bromberg, A.; Schmidt, K. H.; Meisel, D. *J. Am. Chem. Soc.* **1984**, *106*, 3056.
(2) Bromberg, A.; Schmidt, K. H.; Meisel, D. *J. Am. Chem. Soc.* **1985**, *107*, 83.
(3) Nagarajan, V.; Fessenden, R. W. *Chem. Phys. Lett.* **1984**, *112*, 207.
(4) (a) Nagarajan, V.; Fessenden, R. W. *J. Phys. Chem.* **1985**, *89*, 2330. (b) Bhattacharyya, K.; Das, P. K.; Fessenden, R. W.; George, M. V.; Gopidas, K. R.; Hug, G. L. *J. Phys. Chem.* **1985**, *89*, 4164.
(5) Scaiano, J. C.; Tanner, M.; Weir, D. *J. Am. Chem. Soc.* **1985**, *107*, 4396.
(6) Johnston, L. J.; Scaiano, J. C. *J. Am. Chem. Soc.* **1985**, *107*, 6368.
(7) Baumann, H.; Merckel, C.; Timpe, H.-J.; Graness, A.; Kleinschmidt, J.; Gould, I. R.; Turro, N. J. *Chem. Phys. Lett.* **1984**, *103*, 497.
(8) This reaction has actually been observed previously for the perchlorotriphenylmethyl derivative: Luckhurst, G. R.; Ockwell, J. N. *Tetrahedron Lett.* **1968**, *38*, 4123.
(9) Bromberg, A.; Meisel, D. *J. Phys. Chem.* **1985**, *89*, 2507.

0002-7863/86/1508-4706$01.50/0